



HAL
open science

Numerical Simulation of Pseudoelastic Shape Memory Alloys using the Large Time Increment Method

Xiaojun Gu, Ziad Moumni, Wael Zaki

► **To cite this version:**

Xiaojun Gu, Ziad Moumni, Wael Zaki. Numerical Simulation of Pseudoelastic Shape Memory Alloys using the Large Time Increment Method. 13e colloque national en calcul des structures, Université Paris-Saclay, May 2017, Giens, Var, France. hal-01908933

HAL Id: hal-01908933

<https://hal.science/hal-01908933>

Submitted on 30 Oct 2018

HAL is a multi-disciplinary open access archive for the deposit and dissemination of scientific research documents, whether they are published or not. The documents may come from teaching and research institutions in France or abroad, or from public or private research centers.

L'archive ouverte pluridisciplinaire **HAL**, est destinée au dépôt et à la diffusion de documents scientifiques de niveau recherche, publiés ou non, émanant des établissements d'enseignement et de recherche français ou étrangers, des laboratoires publics ou privés.

Numerical Simulation of Pseudoelastic Shape Memory Alloys using the Large Time Increment Method

X. Gu¹, Z. Moumni¹, W. Zaki²

¹ IMSIA, ENSTA-ParisTech, CNRS, CEA, EDF, Université Paris-Saclay, 91120 Palaiseau, France
{xiaojun.gu,ziad.moumni}@ensta-paristech.fr

² Khalifa University, 127788 Abu Dhabi, UAE wael.zaki@kustar.ac.ae

Résumé — The paper presents a numerical implementation of the large time increment (LATIN) method for the simulation of shape memory alloys (SMAs) in the pseudoelastic range. The method was initially proposed as an alternative to the conventional incremental approach for the integration of nonlinear constitutive models. It is adapted here for the simulation of pseudoelastic SMA behavior using the Zaki-Moumni (ZM) model and is shown to be especially useful in situations where the phase transformation process presents little or lack of hardening. In these situations, a slight stress variation in a load increment can result in large variations of strain and local state variables, which may lead to difficulties in numerical convergence. In contrast to the conventional incremental method, the LATIN method solve the global equilibrium and local consistency conditions sequentially for the entire loading path. The achieved solution must satisfy the conditions of static and kinematic admissibility and consistency simultaneously after several iterations. 3D numerical implementation is accomplished using an implicit algorithm and is then used for finite element simulation using the software Abaqus. Numerical results are contrasted to those obtained using step-by-step incremental integration.

Mots clés — large time increment approach ; shape memory alloys ; nonproportional loading ; multiaxial loading ; non-hardening.

1 Introduction

Shape memory alloys (SMAs) are known for their ability to undergo extensive inelastic deformation that can be recovered by heating. The underlying physical mechanism for this ability is a solid-solid phase transformation known as the martensitic transformation. It is responsible for several unusual behaviors observed in SMAs that have promoted their use in engineering applications [3, 4, 5]. A key feature of many SMAs is pseudoelasticity, which refers to the capacity of these materials to deform substantially when subjected to mechanical loading and to recover their undeformed shape once the load is removed. The pseudoelastic behavior of SMAs is the subject of intense investigation in the literature [6, 7, 8, 9, 10, 11, 12, 13, 14, 15, 16, 17], etc.

In [18], Gu *et al.* proposed a numerical integration procedure for the Zaki-Moumni (ZM) model derived in [1] for SMAs subjected to potentially nonproportional multiaxial loading. The implicit time integration procedure was implemented by means of a user material subroutine into the finite element software Abaqus. Despite a marked ability to simulate very complex loading scenarios, convergence difficulties were encountered for SMAs presenting little to no phase transformation hardening. To overcome this issue, we propose an alternative iterative integration algorithm using the so-called “large time increment method” (LATIN) initially introduced in [2]. The method is utilized here for the first time for the integration of constitutive relations for SMAs.

2 Intergration of constitutive relations using LATIN

The state variables used for the derivation of the original ZM model include the total strain ϵ , the temperature T , the volume fraction of martensite z and the local inelastic strain of the martensite phase ϵ^{ori} , which accounts for the detwinning and reorientation of variants. Using these state variables, a Helmholtz free energy is constructed then used to derive constitutive relations consistent with the principles

of thermodynamics. The following stress-strain relation is obtained using this procedure :

$$\boldsymbol{\sigma} = \mathbf{K} : (\boldsymbol{\varepsilon} - z\boldsymbol{\varepsilon}^{\text{ori}}), \quad (1)$$

where $\boldsymbol{\sigma}$ is the stress tensor and \mathbf{K} is the equivalent elastic stiffness tensor, which in general depends on the volume fraction z of martensite.

The above equation reflects that the total inelastic strain in a reference volume element of the SMA is resolved into the product of the amount of martensite that exists within that element and the amount of local inelastic strain experienced by the martensite due to reorientation of the variants. Details of the derivation procedure for the equations reported here can be found in the original publications [1, 12] and a relevant numerical integration algorithm using a conventional operator split and return mapping strategy is provided in [18]. As stated in the introduction, the algorithm was shown to allow proper simulation of SMAs subjected to complex loading but encountered convergence difficulties in situations where the phase transformation plateaus were exceedingly shallow. To overcome this issue, LATIN is used in this paper for the integration of the ZM model. The method involves two major steps :

1. The consistency conditions governing the evolution of the dissipative state variables are relaxed and a solution satisfying the conditions of static equilibrium is obtained for each load increment *for the entire loading path*. The dissipative state variables therefore remain fixed throughout this step,
2. Increments of the dissipative variables are computed for each load increment without enforcing static equilibrium. The solution obtained in this step does not have immediate physical relevance and only serves as an intermediate step in the iterative process.

The two steps are repeated until a solution is achieved that satisfies the conditions of static equilibrium in step 1 and the conditions of consistency in step 2 simultaneously. The main drawback of this iterative procedure is an inferior convergence rate compared to the incremental method using an operator split strategy and an exact material Jacobian, it should therefore be used only in situations where the incremental approach fails to converge because of shallow phase transformation plateaus.

2.1 Initialization

The complete loading history is divided into N increments. At the beginning of the iterative procedure, *i.e.* for $k = 0$ where k denotes the iteration number, all the dissipative variables are set to zero for every load increment n .

$$\forall n \in \{1, \dots, N\}, \quad z_n^{(k=0)} = 0, \quad \boldsymbol{\varepsilon}_n^{\text{ori},(k=0)} = 0. \quad (2)$$

2.2 Enforcing equilibrium

For every load increment n , statically admissible stress fields $\boldsymbol{\sigma}_n^{(k)}$ are computed using values of the dissipative variables from the previous iteration ($k - 1$). These fixed variables introduce an imbalance in the system that is accounted for in solving the boundary value problem for equilibrium. The stress $\boldsymbol{\sigma}_n^{(k)}$ is given by the relation

$$\forall n \in \{1, \dots, N\}, \quad \boldsymbol{\sigma}_n^{(k)} = \mathbf{K}_n^{(k)} \left(\boldsymbol{\varepsilon}_n^{(k)} - z_n^{(k-1)} \boldsymbol{\varepsilon}_n^{\text{ori},(k-1)} \right). \quad (3)$$

Since the only unknown in this case is the statically admissible stress field, this problem is easier to solve than the original one that includes additional requirements of consistency with the loading conditions.

2.3 Enforcing consistency with the loading conditions

Active loading surfaces are detected in this step and the dissipative variables are updated accordingly for each load increment. The increments of the martensite volume fraction $\Delta z_n^{(k)}$ and the inelastic multiplier $\eta_n^{(k)}$ are determined using the following iterative scheme, obtained by solving the linearized

consistency conditions for phase transformation and martensite reorientation :

$$\Delta z^{(m)} = \frac{A_{ori}^{(m)} \mathcal{F}_{ori}^{(m-1)} - B_{ori}^{(m)} \mathcal{F}_z^{(m-1)}}{A_z^{(m)} B_{ori}^{(m)} - B_z^{(m)} A_{ori}^{(m)}}, \quad (4)$$

$$\eta^{(m)} = \frac{B_z^{(m)} \mathcal{F}_z^{(m-1)} - A_z^{(m)} \mathcal{F}_{ori}^{(m-1)}}{A_z^{(m)} B_{ori}^{(m)} - B_z^{(m)} A_{ori}^{(m)}}, \quad (5)$$

where m is the iteration number, \mathcal{F}_z is the loading function for phase transformation and \mathcal{F}_{ori} is the loading function for martensite reorientation. The expressions of the coefficients A and B that appear in equations (4) and (5) can be found in [18].

The increment number n and the iteration number k are eliminated from the above equations for readability.

Upon convergence, the stress is determined $\forall n \in \{1, \dots, N\}$ using the relation

$$\hat{\boldsymbol{\sigma}}_n^{(k)} = \mathbf{K}_n^{(k)} \left(\boldsymbol{\varepsilon}_n^{(k)} - z_n^{(k,M)} \boldsymbol{\varepsilon}_n^{\text{ori},(k,M)} \right), \quad (6)$$

in which M is the iteration number m at convergence.

2.4 Error and stopping criteria

At the end of each iteration $k + 1/2$ over the complete loading path, a residual \mathcal{R} is computed using the relation

$$\mathcal{R} = \frac{1}{T} \sum_{t=1}^T \max_{1 \leq n \leq N} \frac{\|\hat{\boldsymbol{\sigma}}_n^{(k)} - \boldsymbol{\sigma}_n^{(k)}\|}{\|\hat{\boldsymbol{\sigma}}_n^{(k)}\| + \|\boldsymbol{\sigma}_n^{(k)}\|}, \quad (7)$$

where $\boldsymbol{\sigma}_n^{(k)}$ and $\hat{\boldsymbol{\sigma}}_n^{(k)}$ are given by equations (3) and (6), t is the integration point number in the simulated FE model and T is the number of integration points. The iterative process is stopped when \mathcal{R} becomes sufficiently small.

3 Algorithmic setup

A ‘‘User Material’’ subroutine (UMAT) is developed for the integration of the constitutive equations of the ZM model using LATIN in the finite element analysis software Abaqus. The iterative process described in the previous section is implemented by means of Python scripts and repeated until the stopping condition in the previous section is met. The subroutine itself uses the implicit integration algorithm presented below in order to update the stress components and the local state variables separately at the end of each load increment in a given iteration covering a complete loading path. The parameters tol_1 and tol_2 that appear in the algorithm are numerical tolerances.

1. Read the parameters of the model and discretize the loading path ;
2. Determine the stress field $\boldsymbol{\sigma}_n^{(k)}$ for load increment n at iteration k using equation (3) ;
3. If $\mathcal{F}_{z,n}^{(k,0)} \leq tol_1$ and $\mathcal{F}_{ori,n}^{(k,0)} \leq tol_1$, the stress solution is acceptable. Set the state variables to their values at the previous iteration for the same load increment,

$$z_n^{(k)} = z_n^{(k-1)} \text{ and } \boldsymbol{\varepsilon}_n^{\text{ori},(k)} = \boldsymbol{\varepsilon}_n^{\text{ori},(k-1)} ;$$

4. Else if $\mathcal{F}_{z,n}^{(k,0)} > tol_1$ or $\mathcal{F}_{ori,n}^{(k,0)} > tol_1$:
 - (a) Determine the increment $\Delta z_n^{(k)}$ of the martensite volume fraction and the increment $\eta_n^{(k)}$ of the inelastic multiplier using equations (4) and (5),
 - (b) Update the state variables $z_n^{(k)}$ and $\boldsymbol{\varepsilon}_n^{\text{ori},(k)}$;
5. Compute the residual \mathcal{R} ;
6. Check for convergence :
 - (a) If $n = N$ (i.e. at the last increment), then

- i. If $\mathcal{R} \leq tol_2$ (convergence) then end,
- ii. Else
 - Set $k = k + 1$ and $n = 1$ and go to 2;
- (b) Else
 - Set $n = n + 1$ and go to 2.

4 Results and discussion

The UMAT in the previous section is used to simulate a single hexahedral SMA element subjected to different loading cases and a SMA plate with a hole in the center subjected to alternating pressure.

Parameter	Value	Parameter	Value
E_A	30340 MPa	a	2.84 MPa
E_M	18000 MPa	b	2.84 MPa
ν	0.3	ϵ_0	0.03
Y	30 MPa	G	0.9 MPa
α	666.67 MPa	β	1666.67 MPa
ξ	0.26 MPa K ⁻¹	κ	2.09 MPa
A_f^0	320 K	T	340 K

TABLE 1 – Material parameters used for the simulation of the SMAs subjected to uniaxial tension.

4.1 SMA element subjected to uniaxial tension

A single hexahedral SMA element is subjected to tension that increases monotonically from 0 to 800 MPa. The reference stress-strain curve for the material is reported in Figure 1(b) and shows perfectly flat phase transformation plateaus. The simulation completes in this case in 12 iterations using the parameters in Table 1 and a tolerance of 0.4% on the residual \mathcal{R} . Additional iterations are required if a smaller tolerance is desired.

As shown in Figure 1(a), the computed stress-strain curve starts perfectly linear then gradually approaches the reference curve in subsequent iterations until a converged solution is obtained as illustrated in Figure 1(b).

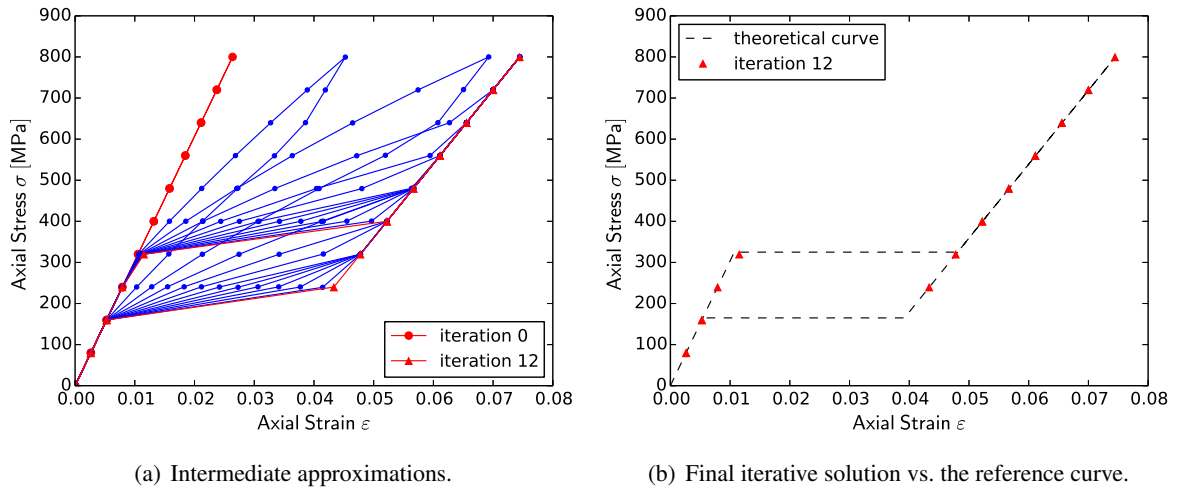


FIGURE 1 – Stress-strain curve.

4.2 SMA element subjected to multiaxial loading

The three loading cases in Figure 2 are considered in this section. In the figure, path 1 corresponds to pure tension, path 2 to pure shear, and path 3 is a combination of both. The simulations are performed

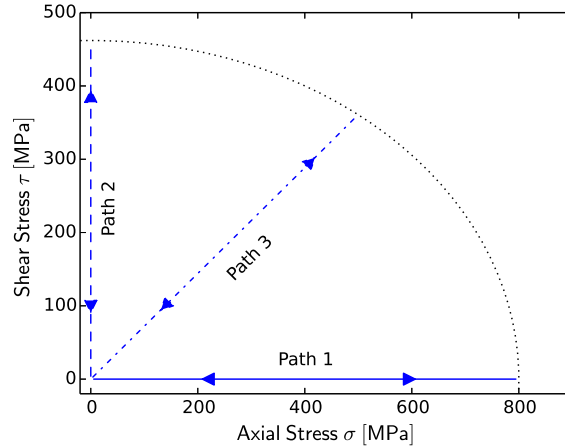


FIGURE 2 – Stress-controlled proportional loading.

on a single fully integrated 8-node hexahedral element (Abaqus designation C3D8) up to a maximum von Mises equivalent stress of 800 MPa in each case. A constant temperature $T = 340\text{ K}$ is considered for which the shape memory alloy is pseudoelastic. The parameters used for the simulations are listed in Table 2 and the tolerance on the residual \mathcal{R} is set to 1%. 18 iterations were required for convergence in this case. Intermediate approximations of the stress-strain behavior using LATIN are shown in Figure 3(a) for loading case 1. The comparison of the converged solution with the one obtained using the conventional incremental algorithm in [18] is shown in Figure 3(b). Similar results are reported in

Parameter	Value	Parameter	Value
E_A	30340 MPa	a	5.16 MPa
E_M	18000 MPa	b	6.36 MPa
ν	0.3	ϵ_0	0.04
Y	30 MPa	G	13.17 MPa
α	500 MPa	β	1250 MPa
ξ	0.20 MPa K ⁻¹	κ	4.16 MPa
A_f^0	320 K	T	340 K

TABLE 2 – Material parameters used for the simulation of the SMAs subjected to multiaxial loading.

Figures 4(a) to 5(b) for the second and third loading cases.

It is clear from the figures that the results obtained with the iterative algorithm using LATIN perfectly fit those obtained using the algorithm in [18].

4.3 Simulation of a SMA plate with a hole in the center

The rectangular SMA plate in Figure 6(a) is considered in this section. The plate is $100 \times 120 \times 15\text{ mm}^3$ in size and contains a hole in the center 25 mm in radius. It is subjected to the biaxial loading shown in Figures 6(a) and 6(b). In this case, the material parameters used are those in Table 1, for which the phase transformation plateaus are perfectly flat.

Using the algorithm in [18], the simulation aborted at time step 0.88 because of convergence difficulty. However, using the LATIN-based algorithm, the simulation completes in 60 iterations with a tolerance of 0.1% on the residual \mathcal{R} and the total solution time was 28 minutes. The computed distributions of von Mises stress and the volume fraction of martensite in the plate are reported in Figure 7 for time step 0.5 at which surface tractions $P1$ and $P2$ are both maximal.

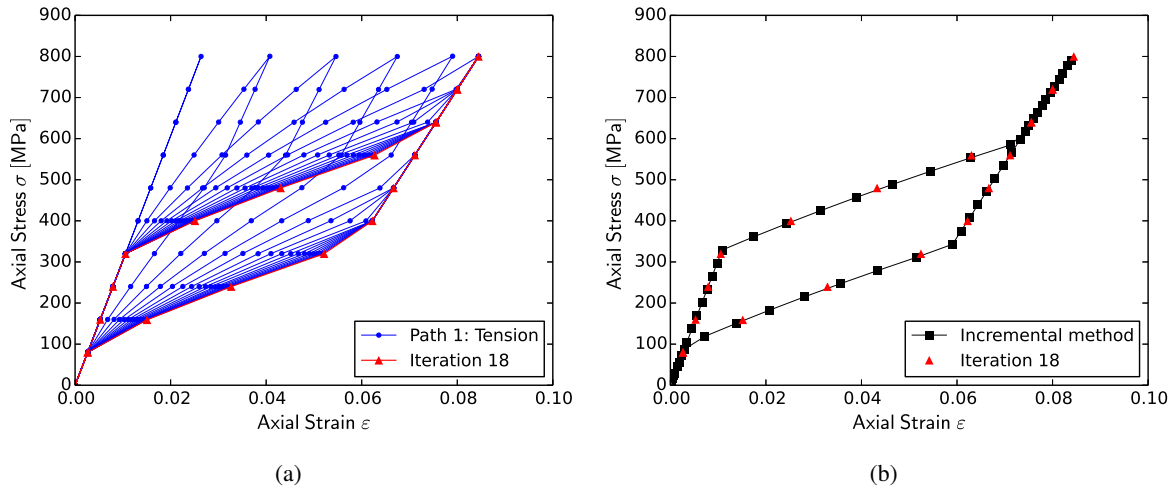


FIGURE 3 – Simulated stress-strain behavior for the case of uniaxial tension.

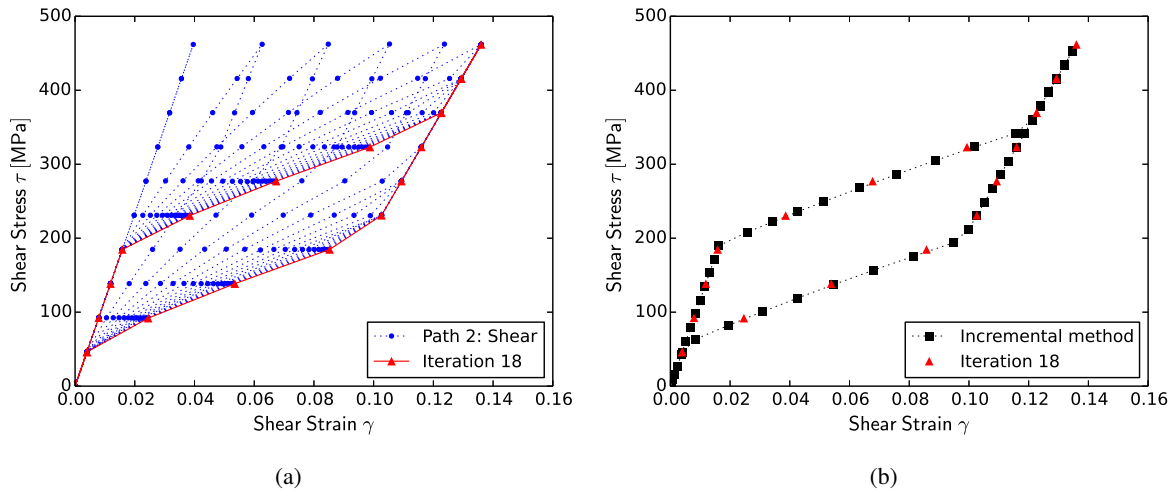


FIGURE 4 – Simulated stress-strain behavior for the case of pure shear.

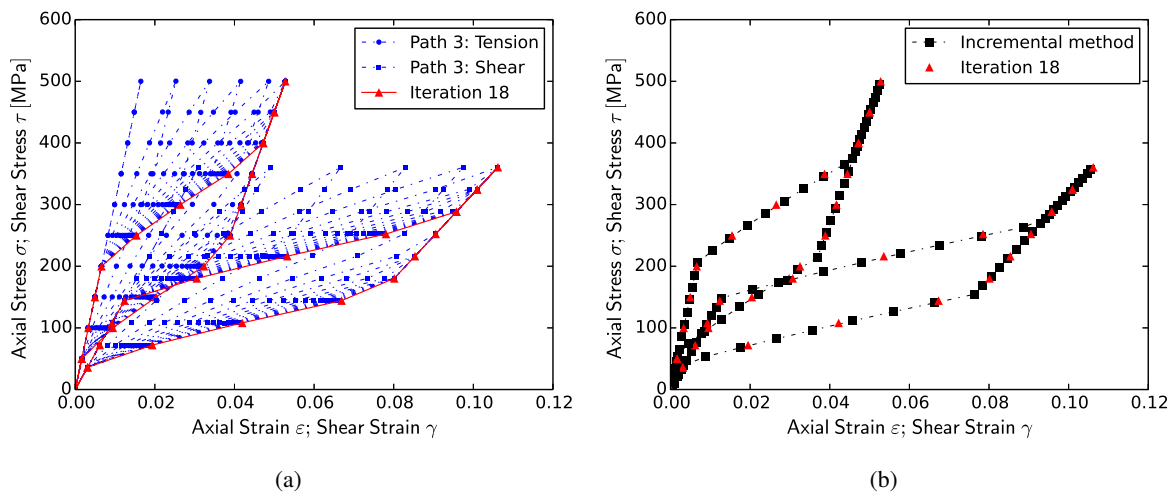


FIGURE 5 – Simulated stress-strain behavior in tension and in shear for the case of combined loading.

The results include the von Mises stress distribution in Figure 7(a) and the corresponding distribution of the martensite volume fraction in the sample in Figure 7(b). It is worth noting that values of the volume fraction reported outside the interval $[0, 1]$ are a result of the data interpolation carried out by Abaqus in representing the volume fraction contours. The actual values, computed at individual integration points, are well within the acceptable range to a user-specified numerical tolerance.

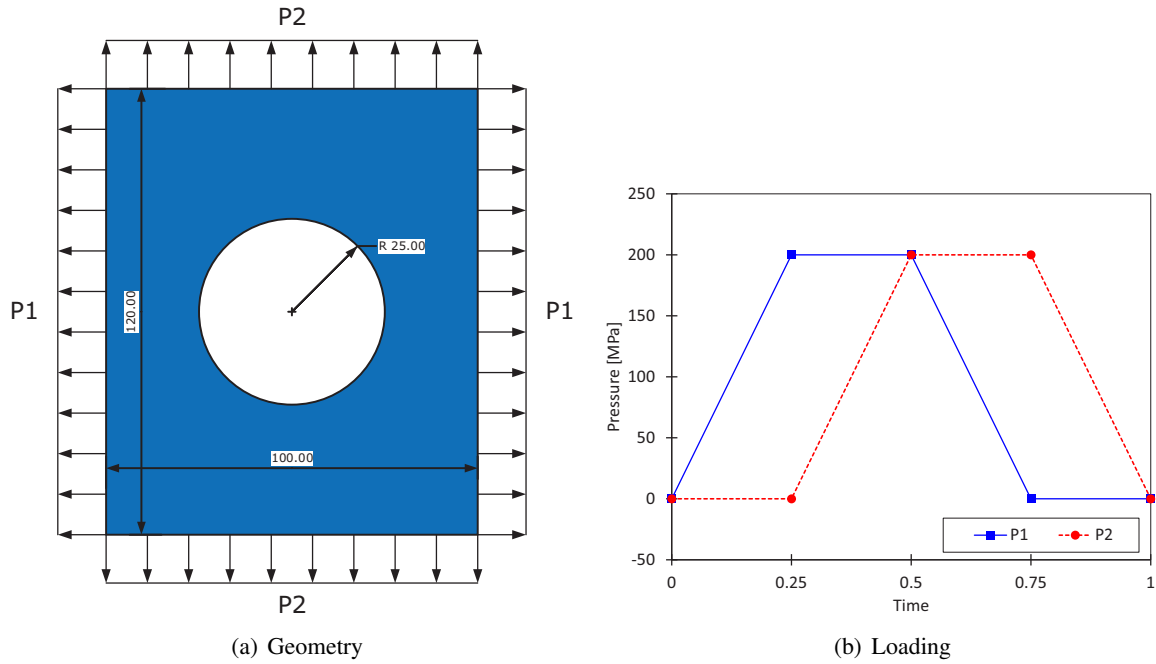


FIGURE 6 – Geometry and loading of a plate with a hole in the center.

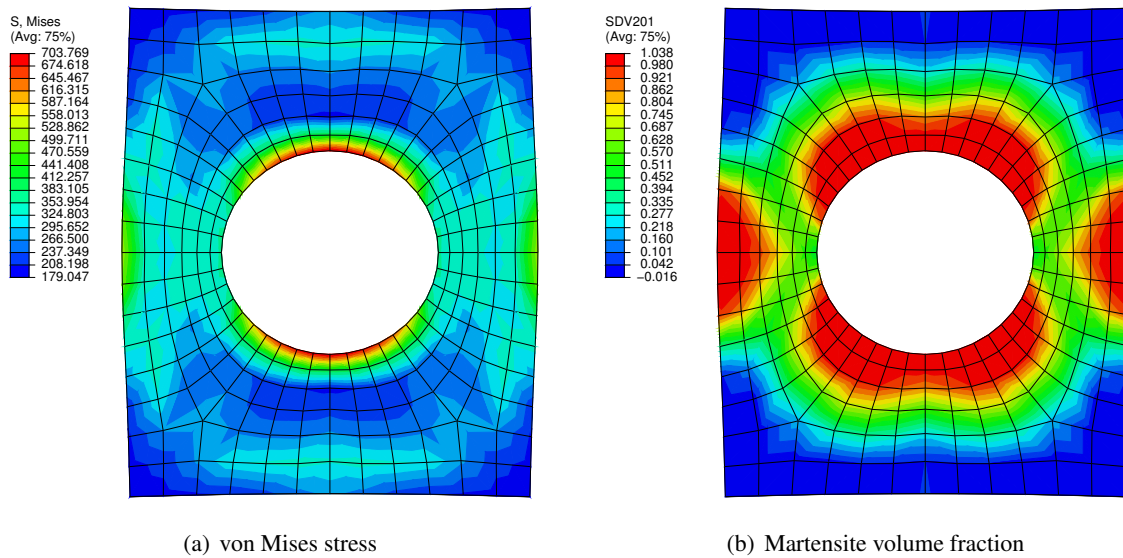


FIGURE 7 – Simulation results at time step of 0.5.

5 Conclusion

An implementation of the Large Time Increment method for the integration of the constitutive equations of the ZM model was presented for the first time in this paper. The method was programmed into a user material subroutine (UMAT) that was used in several finite element simulations in Abaqus. The UMAT was successful in simulating the behavior of shape memory alloys presenting flat phase transformation plateaus, including samples with complex geometries subjected to nonproportional loading. It was also shown to provide results consistent with those obtained using the conventional incremental algorithm in [18] for loading cases in tension and shear.

Références

- [1] Zaki, W., and Mousni, Z., 2007. “A three-dimensional model of the thermomechanical behavior of shape memory alloys”. *Journal of the Mechanics and Physics of Solids*, **55**(11), pp. 2455–2490.

- [2] Boisse, P., Bussy, P., and Ladeveze, P., 1990. “A new approach in non-linear mechanics : The large time increment method”. *International Journal for Numerical Methods in Engineering*, **29**(3), Mar., pp. 647–663.
- [3] Van Humbeeck, J., 1999. “Non-medical applications of shape memory alloys”. *Materials Science and Engineering : A*, **273-275**, Dec., pp. 134–148.
- [4] Hartl, D. J., and Lagoudas, D. C., 2007. “Aerospace applications of shape memory alloys”. *Proceedings of the Institution of Mechanical Engineers, Part G : Journal of Aerospace Engineering*, **221**(4), pp. 535–552.
- [5] Duerig, T., Pelton, A., and Stöckel, D., 1999. “An overview of nitinol medical applications”. *Materials Science and Engineering : A*.
- [6] Brinson, L., and Lammering, R., 1993. “Finite element analysis of the behavior of shape memory alloys and their applications”. *International Journal of Solids and Structures*, **30**(23), Jan., pp. 3261–3280.
- [7] Sittner, P., Hara, Y., and Tokuda, M., 1995. “Experimental study on the thermoelastic martensitic transformation in shape memory alloy polycrystal induced by combined external forces”. *Metallurgical and Materials Transactions A*, **26**(11), pp. 2923–2935.
- [8] Lim, T. J., and McDowell, D. L., 1999. “Mechanical Behavior of an Ni-Ti Shape Memory Alloy Under Axial-Torsional Proportional and Nonproportional Loading”. *Journal of Engineering Materials and Technology*, **121**(1), pp. 9–18.
- [9] Bouvet, C., Calloch, S., and Lexcellent, C., 2002. “Mechanical Behavior of a Cu-Al-Be Shape Memory Alloy Under Multiaxial Proportional and Nonproportional Loadings”. *Journal of Engineering Materials and Technology*, **124**(2), pp. 112–124.
- [10] Auricchio, F., Taylor, R. L., and Lubliner, J., 1997. “Shape-memory alloys : macromodelling and numerical simulations of the superelastic behavior”. *Computer Methods in Applied Mechanics and Engineering*, **146**(3–4), pp. 281–312.
- [11] Bo, Z., and Lagoudas, D. C., 1999. “Thermomechanical modeling of polycrystalline SMAs under cyclic loading, Part I : theoretical derivations”. *International Journal of Engineering Science*, **37**(9), pp. 1089–1140.
- [12] Zaki, W., and Moumni, Z., 2007. “A 3D model of the cyclic thermomechanical behavior of shape memory alloys”. *Journal of the Mechanics and Physics of Solids*, **55**(11), pp. 2427–2454.
- [13] Moumni, Z., Zaki, W., and Nguyen, Q. S., 2008. “Theoretical and numerical modeling of solid–solid phase change : Application to the description of the thermomechanical behavior of shape memory alloys”. *International Journal of Plasticity*, **24**(4), pp. 614–645.
- [14] Morin, C., Moumni, Z., and Zaki, W., 2011. “Direct Numerical Determination of the Asymptotic Cyclic Behavior of Pseudoelastic Shape Memory Structures”. *Journal of Engineering Mechanics*, **137**(7), pp. 497–503.
- [15] Ould Moussa, M., Moumni, Z., Doaré, O., Touzé, C., and Zaki, W., 2012. “Non-linear dynamic thermomechanical behaviour of shape memory alloys”. *Journal of Intelligent Material Systems and Structures*.
- [16] Zaki, W., Moumni, Z., and Morin, C., 2011. “Modeling tensile-compressive asymmetry for superelastic shape memory alloys”. *Mechanics of Advanced Materials and Structures*, **18**(7), pp. 559–564.
- [17] Zaki, W., 2012. “Time integration of a model for martensite detwinning and reorientation under nonproportional loading using Lagrange multipliers”. *International Journal of Solids and Structures*, **49**(21), pp. 2951–2961.
- [18] Gu, X., Zaki, W., Morin, C., Moumni, Z., and Zhang, W., 2014. “Time Integration and Assessment of a Model for Shape Memory Alloys Considering Multiaxial Nonproportional Loading Cases”. *International Journal of Solids and Structures*, Nov.